Heliyon 8 (2022) e11023

Contents lists available at ScienceDirect

Heliyon

journal homepage: www.cell.com/heliyon

Research article

Comparison and critical assessment of single-cell Hi-C protocols

M. Gridina [a,1], A. Taskina [a,1], T. Lagunov [a,b], A. Nurislamov [a,b], T. Kulikova [c], A. Krasikova [a,c], V. Fishman [a,b,d,*]

[a] Institute of Cytology and Genetics SB RAS, Novosibirsk, Russia
[b] Novosibirsk State University, Novosibirsk, Russia
[c] Laboratory of Nuclear Structure and Dynamics, Cytology and Histology Department, Saint Petersburg State University, Saint Petersburg, Russia
[d] AIRI, Moscow, Russia

ARTICLE INFO

Keywords:
Single-cell Hi-C
Genome architecture
Chicken
Oocyte

ABSTRACT

Advances in single-cell sequencing technologies make it possible to study the genome architecture in single cells. The rapid growth of the field has been fueled by the development of innovative single-cell Hi-C protocols. However, the protocols vary considerably in their efficiency, bias, scale and costs, and their relative advantages for different applications are unclear.

Here, we compare the two most commonly used single-cell Hi-C protocols. We use long-read sequencing to analyze molecular products of the Hi-C assay and show that whole-genome amplification step results in increased number of artifacts, larger coverage biases, and increased amount of noise compared to PCR-based amplification. Our comparison provides guidance for researchers studying chromatin architecture in individual cells.

1. Introduction

Chromatin architecture plays an important role in genome biology. Hi-C is one of the most common techniques employed to study chromatin organization in the nucleus. Multiple modifications of Hi-C protocol were developed to study genome architecture (Kempfer and Pombo, 2020), yet most of them require large amount of input material and therefore cannot be applied to study individual cells.

Single cell analysis is essential when pure subpopulations cannot be isolated or when obtaining large amount of cells is challenging. Typical examples of such rare cell populations are oocytes and early embryonic cells (Flyamer et al., 2017; Díaz et al., 2018; Zhang et al., 2020). Recently, several single-cell Hi-C (scHi-C) protocols have been proposed to address this challenge. The key difference between these protocols is a strategy of DNA amplification. There are PCR-based whole-genome amplification methods including degenerate oligonucleotide-primed PCR, primer extension PCR and ligation-mediated PCR. They generate low molecular weight DNA (less than 1500 bp) with incomplete genome coverage and amplification bias (Dean et al., 2002; Huang et al., 2015). On the other hand, multiple displacement amplification (MDA) is based on using random hexamer primers and strand-displacement polymerases which work at a constant temperature, that allow obtaining high molecular weight DNA. In addition, some MDA methods use phi29 DNA polymerase with proofreading activities that increase sequence fidelity. Although MDA results in better genome coverage than PCR-based methods (Huang et al., 2015), the main weakness is uneven coverage including the high allele dropout rate (Borgström et al., 2017) and overamplification of some regions (Chen et al., 2014).

The scHi-C protocol developed by Flyamer et al. (2017) employs MDA of proximity ligation products. On the other hand, Nagano et al. (2017) employs a ligation-mediated PCR method at the stage of NGS library amplification.

Due to different amplification strategy, MDA-protocols do not allow enrichment of proximity ligation products; in addition, these protocols differ in DNA fragmentation methods (see Table 1 to review key differences of scHi-C methods.

Here, we compared two basic subtypes of scHi-C protocol suitable for the analysis of rare cell populations: MDA- and PCR-based. We found that PCR-based amplification generates more uniform coverage and reduced number of artifacts compared to phi29-based amplification. Using long-read sequencing of phi29-derived products, we showed that phi29-amplification results in circular DNA overamplification and template switching, which explains many of the observed artifacts.

* Corresponding author.
E-mail address: minja-f@ya.ru (V. Fishman).
[1] Equal contribution.

https://doi.org/10.1016/j.heliyon.2022.e11023
Received 18 June 2022; Received in revised form 13 August 2022; Accepted 6 October 2022

2. Methods

2.1. Nuclei isolation and formaldehyde fixation

Chicken oocytes with a diameter from 1 to 2 mm were dissected from the ovary and placed in individual drops of cooled "5:1" medium (83 mM KCl, 17 mM NaCl, 6.5 mM Na_2HPO_4, 3.5 mM KH_2PO_4, 1 mM $MgCl_2$, 1 mM DTT, pH 7.2). Nuclei were isolated as previously published (Krasikova et al., 2012), washed with "5:1" medium and transferred for fixation into a dish containing 2% formaldehyde in PBS for 15 min at room temperature. Formaldehyde was quenched with 0.125 M glycine during 15 min at room temperature. The nuclei integrity was estimated under Olympus stereomicroscope. The Hi-C protocol was proceeded immediately.

All animal experiments were approved by the bioethics committee of the Institute of Cytology and Genetics SB RAS (Protocol N⁰66, October 9th, 2020). International guidelines were followed during experimental procedures ("Guide for the Care and Use of Laboratory Animals" (National Research Council, 2011)).

2.2. Single-nucleus Hi-C

Two Hi-C protocols were used in this study

The first one - MDA-based. We applied the previously described protocol by Flyamer et al. (2017) with some modifications.

Individual fixed nuclei were transferred into wells of microplate with a 9 μL ice-cold lysis buffer (10 mM Tris-HCl pH 8.0, 10 mM NaCl, 0.2% Igepal) for 30 min. Nuclei were washed with NEB3.1 + 0.5% SDS, and incubated with NEB3.1 + 0.5% SDS for 2 h at 37° with shaking. Then each of the nuclei was washed with NEB3.1 + 3% Triton X-100. Chromatin fragmentation was performed with 25U DpnII (New England Biolabs) at 37 °C overnight. Nuclei was washed with T4 ligase buffer NEB and incubated with T4 ligase at 16 °C overnight. Cross-links were reversed by incubating at 65 °C overnight and Low Melting Point Agarose was digested by 0.4U Agarase (Thermo Fisher Scientific) 1 h at 42 °C. DNA from each nucleus was purified with AMPure XP magnetic beads and amplified using illustra GenomiPhi v2 DNA amplification kit strictly according to (Kumar et al., 2008). DNA was purified and sheared to a size of 200–400 bp using focused-ultrasonicator Covaris M220. The following parameters were used: duty factor, 20; peak power, 50; cycles per burst, 200; and time, 110 s. NGS libraries were prepared with KAPA HyperPrep kit with KAPA single-indexed adapter kit set A and B according to the manufacturer manual. 4 cycles of PCR library amplification were performed. Two samples were prepared for ONT sequencing according to the manufacturer manual. The second one was PCR-based.

The main differences from the previous one were using:

- UltraPure™ Low Melting Point Agarose (Thermo Fisher Scientific) to avoid nuclei loss;
- biotine-dCTP for the enrichment of the ligation products;
- AluI for fragmentation of DNA for NGS libraries preparation;
- 25 cycles of PCR.

Table 1. List of key scHi-C protocols.

Article	Key protocol features
Flyamer et al. (2017)	Multiple displacement amplification (MDA); Sonication
Nagano et al. (2017)	PCR-based; Tagmentation of ligated DNA, Biotin enrichment
Collombet et al. (2020)	PCR-based; Tagmentation of ligated DNA; Biotin enrichment
Stevens et al. (2017)	PCR-based, AluI digestion of ligated DNA; Biotin enrichment
Tan et al. (2018)	Multiplex end-tagging amplification of ligated DNA
Ke et al. (2017)	PCR-based; Biotin enrichment
Ulianov et al. (2021)	Multiple displacement amplification (MDA); Sonication

Individual fixed nuclei were transferred into wells of microplate with a 9 μL ice-cold lysis buffer for 20 min. Nuclei were washed with NEB3.1 + 0.5% SDS, and moved to 0.2 ml PCR tubes with the 3 μL NEB3.1 + 0.5% SDS. 10 μL fresh prepared 1.2% Low Melting Point Agarose were added into each tube with control under the stereomicroscope. After solidification 10 μL NEB3.1 + 0.6% SDS were added and samples were incubated 1 h at 37 °C. 10 μL 6% Triton X-100 were used for SDS quenching and chromatin fragmentation was performed with 25U DpnII (New England Biolabs) at 37 °C for overnight. The digested chromatin ends labeling was performed by 5 U Klenow fragment in the presence of biotin-15-dCTP at 22 °C for 4 h followed by ligation at 16 °C overnight. Crosslinks were reversed by incubating at 65 °C overnight and Low Melting Point Agarose were digested by Agarase (Thermo Fisher Scientific) 1 h at 42 °C. Purified DNA was fragmented by AluI 1 h at 37 °C and NGS libraries were prepared with KAPA HyperPrep kit according to the manufacturer manual with some modifications. The volumes of end repair, adapter ligation reactions and PCR were reduced by 5, 5 and 2 times, respectively. The adapters were diluted to 300 nM. There was biotin pull-down with Dynabeads MyOne Streptavidin T1 beads after the adapter ligation step. 25 cycles of PCR were performed.

2.3. Bioinformatic analysis

ONT-data was processed using Pore-C-Snakemake. For bioinformatics analysis of ONT libraries we used the output of the Pore-C-Snakemake program (version 0.2.0), specifically files from merged_contacts and align_table directories. Merged_contact directory contains files with a list of Hi-C contacts. Align_table directory contains the list of aligned fragments of ont-reads.

For analysis of Illumina libraries, we followed the protocol described in Fishman et al. (2019): we used the output of the Juicer program, specifically the files from merged_nodups.txt. This file contains the list of the Hi-C contacts after all preprocessing procedures. The ratio of intrafragment reads has been subtracted directly from output Juicer file – stats. txt, which contains performance indicators of the runned analysis. All files have been read as pandas dataframe, further statistical analysis has been done using standard python libraries – pandas, numpy, scipy. We also used python packages matplotlib and seaborn for visualization.

We used the following Hi-C ligation motifs: *GATC* for MDA protocol (this sequence is generated after re-ligation of the DpnII cut sites); GATCGATC for PCR protocol (this sequence is generated after fill-in and ligation of the DpnII cut sites).

To evaluate the number of dangling ends (DE), we used the following equation:

$$DE = (FR + RF) - (FF + RR)$$

where FR, RF, FF, and RR are the number of valid pairs with read mates in the forward–reverse, reverse–forward, forward–forward and reverse–reverse orientations, respectively. It was assumed that the FR, RF, FF and RR classes of the Hi-C read orientations were distributed at a ratio of 1:1:1:1 and that overrepresentations of FR or RF might indicate the presence of either non-ligated fragments or back ligations.

Rings ratio (RR) was obtained by dividing total number of the aligned read base pairs (Aligned) by total length of unique reference regions (Unique) covered by this read and subtracting obtained ratio from 1: RR = 1 − Unique/Aligned.

Rings ratio equal to zero indicates that each alignment block reported for the read is unique and does not overlap with other alignment blocks, whereas rings ratio close to one indicates that alignment blocks are highly overlapping.

Randomized controls of reads ratio were obtained by randomly permuting positions of reads.

3. Results and discussion

3.1. PCR-based amplification generates better single-cell Hi-C libraries compared to MDA-based protocols

As a part of the large project focused on the analysis of chicken oocytes epigenome, we prepared single-cell Hi-C libraries from nuclei of chicken oocytes using two different library preparation methods: MDA- and PCR-based (Figure 1). Single cell technique was chosen because large number of oocytes cannot be isolated. Although we note that studying chromatin organization in these cells is important, we limit the current study to the comparison of Hi-C protocols.

We sequenced nine libraries prepared with the MDA-based protocol and 15 libraries prepared using PCR-based protocol. The details of these protocols are provided in the "Methods" section, but here we briefly review the key differences between them. Both protocols begin with nucleus isolation, formaldehyde fixation, and in-chromatin digestion with DpnII enzyme (Figure 1). The PCR-based protocol continues with DNA ends biotinylation and ligation, DNA fragmentation, biotin pull-down which allows enrichment of ligation products, adapter ligation, and PCR-amplification. For MDA-based protocol, we amplified DNA after the ligation step using phi29 enzyme, which has a strand-displacement activity, fragmented the obtained library using sonication, and continued with adapter ligation, DNA amplification, and Illumina sequencing.

Using sequencing data, we accessed several key statistics of Hi-C libraries. First, we computed the number of intra-fragment read pairs, representing DNA fragments that failed to ligate. We found that MDA-based protocol results in 4–5 times more intra-fragment reads than PCR-based protocol (Figure 2A). We assumed that this difference is because in the MDA-based protocol, there is no enrichment of proximity ligation products. In accord with the increase of intra-fragment reads, for MDA-based libraries, we observed more reads in FR-orientation, which often (although not always - Gridina et al., 2021) inversely correlate with the number of proximity ligation products (Figure 2A). Finally, we note that both MDA- and PCR-based libraries are PCR-amplified after DNA

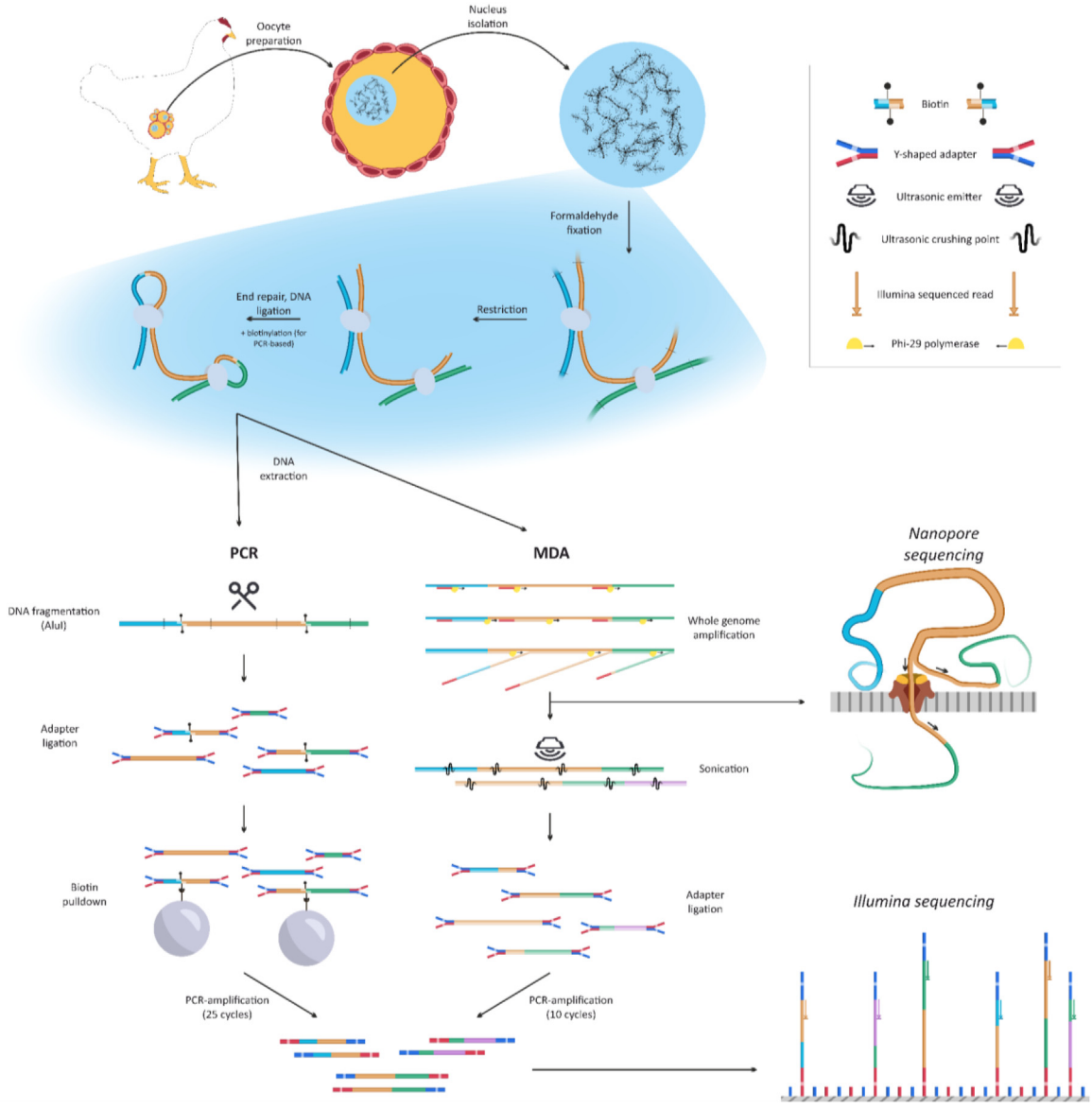

Figure 1. Two protocols of single-cell Hi-C library preparation benchmarked in this study. Both methods include nucleus isolation, nucleus fixation, chromatin restriction, DNA ends repair and ligation. PCR-based protocol continues with AluI-digestion, biotin pull-down, adapter ligation, amplification and Illumina sequencing. MDA-based protocol includes phi29-amplification followed either by direct ONT-sequencing or sonication, adapter ligation, PCR amplification and Illumina sequencing.

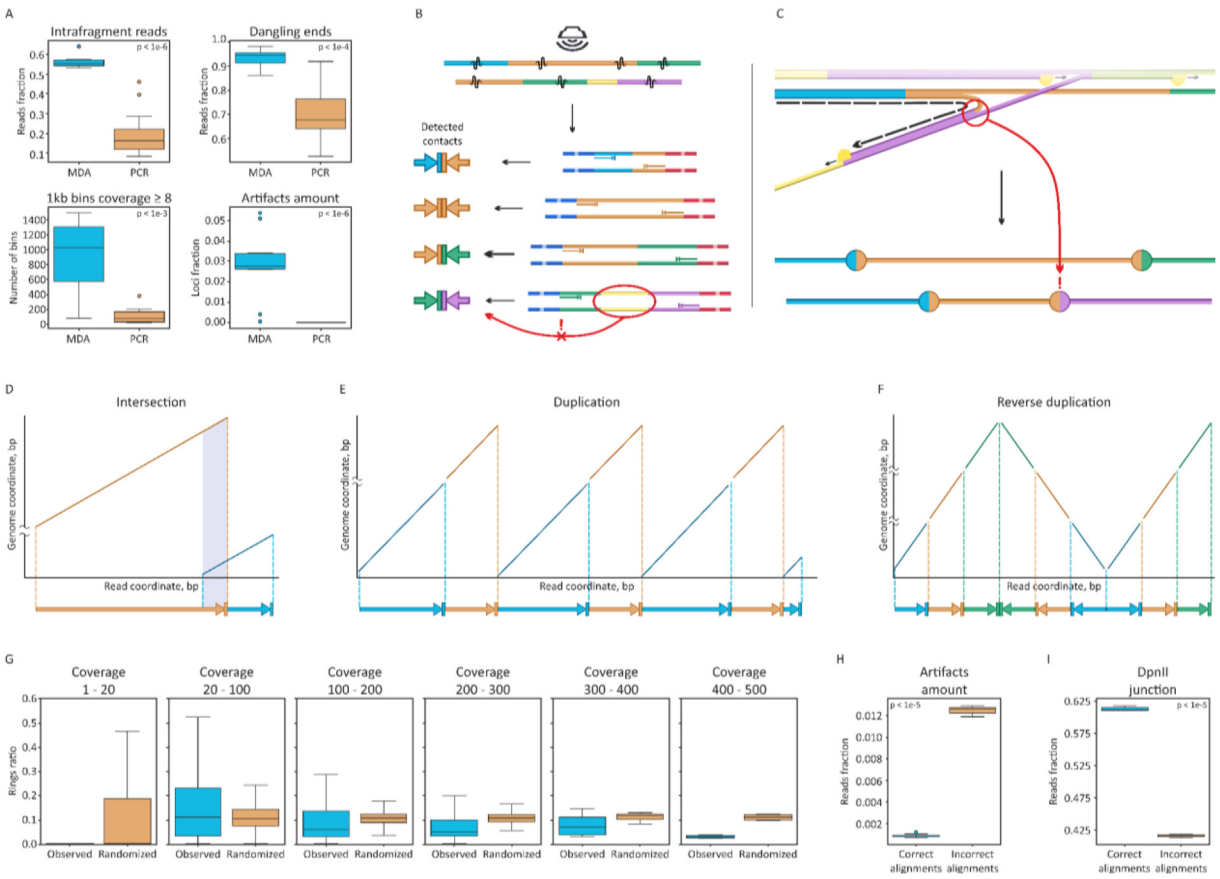

Figure 2. Comparison of scHi-C protocols. A. Quality metrics for PCR- and MDA-based protocols. B and C. Illustration of two hypotheses explaining artifacts observed in scHi-C data. D-F. Representations of different alignment types observed in long-read sequencing data. Graphs represent real alignment results observed in the data. G. Interdependence of genomic coverage of loci and rings ratio of the reads overlapping them. Data presented as boxplots showing the distribution of rings ratio for each genomic coverage strata. Briefly, rings ratio equal to zero indicates that each alignment block reported for the read is unique and does not overlap with other alignment blocks, whereas rings ratio close to one indicates that alignment blocks are highly overlapping. The details of rings ratio and randomized controls are provided in methods section. H. Fraction of artifacts shown for reads characterized by consistent and inconsistent alignments. I. Fraction of artifacts shown for reads with or without DpnII junctions. For A, I and H, samples represent individual oocyte nuclei, p-values obtained using Mann-Whitney U-test.

fragmentation and adapter ligation steps, and aimed to estimate library complexity after this final round of amplification. We found that coverage distribution was more uniform for PCR-based libraries, whereas in MDA-based libraries several loci showed unexpectedly high sequencing coverage (Figure 2A).

Interestingly, some restriction fragments within these highly covered regions displayed numerous interactions, whereas we expected not more than eight interactions to be observed for each restriction fragment, i.e. four (number of chromatids in meiotic oocyte) * 2 (ends of each fragment) (Galitsyna and Gelfand, 2021). We defined restriction fragments detected in more than eight different chimeric DNA fragments as artifacts and counted the number of artifacts for each of the obtained libraries. To compare this statistic across samples, we downsampled all datasets to 20 000 read pairs to remove a factor of sequencing depth. This analysis shows that the number of artifacts was substantially higher for MDA-based libraries than for PCR-based (Figure 2A).

3.2. Artifacts in MDA-based libraries arise from circular fragments overamplification and template switching

We proposed two alternative hypotheses explaining artifacts of the MDA-based protocol (Figure 2B and C).

First, random fragmentation of identical long molecules may produce short fragments containing different pairs of restriction fragments on their ends (Figure 2B). These different short fragments are interpreted as independent Hi-C-contacts, although they represent MDA duplicates of the single long proximity ligation product. This leads to an overestimation of contact counts and loci proximity. Second, phi29 polymerase may switch templates during amplification (Lasken and Stockwell, 2007), generating new DNA junctions which are erroneously interpreted as products of proximity ligation (Figure 2C).

To score the importance of these two sources of artifacts and to explain why some loci display abnormally high coverage after MDA, we employed Oxford Nanopore long-read technology (ONT). We split all material obtained after MDA into two aliquots, one sequenced directly using ONT, and another subjected to sonication, adapter ligation, and Illumina short-read sequencing (Figure 1). This allowed us to directly compare Hi-C statistics obtained for short- and long-read sequencing.

We examined ONT-read alignments within the regions displaying abnormally high coverage. Typical ONT-reads contain junctions of several genomic fragments, which often concur with DpnII cut sites. However, in regions displaying high coverage, we observed reads containing multiple repeats of individual DpnII restriction fragments (Figure 2E and F). Frequently, but not always, the order of the fragments within the read was unchanged, i.e. the same chain of segments was repeated multiple times (Figure 2E). However, we also observed cases when the chain of fragments was reordered, i.e. a single read contained genomic segments A, B and C ordered as A–B–C–C–B–A (Figure 2F).

We interpret these repetitive chains of fragments as products obtained by amplification of circular templates, generated during the proximity ligation step. Quantitative analysis also confirmed that the portion of circular products significantly increases at regions with high genomic

coverage, i.e. regions where read coverage exceeds 200 (Figure 2G). We assumed that reordering of segments arises from polymerase template switching, as described in Lasken and Stockwell (2007).

To sum up, we concluded that MDA amplification results in unequal reads coverage due to the overamplification of circular products. Template switching during amplification of circular templates produces artifacts that do not represent proximity ligation events.

We next aimed to explore other sources of artifacts in the MDA-derived scHi-C data. For this aim, we explored alignments of the ONT reads, which supported contacts of fragments with more than eight contacts. We found that these reads often contain inconsistent alignment segments, which we defined as alignment segments with sharing some fraction of read sequence (Figure 2D) or alignment segments separated by a large unaligned gap. Filtering out overlapping alignments or segments separated by a large ($\geq$ 10 bp) unaligned gap significantly reduced the number of artifacts (Figure 2H). Moreover, we found that DpnII cut sites, which are expected at Hi-C ligation junctions, coincide with the ends of consistent alignment segments significantly more often than with the ends of inconsistent alignment segments. Filtering our reads without DpnII cut sites near alignment segment junctions also significantly reduced the number of artifacts (Figure 2I). Thus, we concluded that erroneous alignment is an important source of artifacts in ONT-derived Hi-C data. Interestingly, analysis of the same MDA library subjected to sonication and Illumina sequencing with the matched total number of contacts showed a substantially lower number of artifacts, indicating that erroneous alignments are mainly an issue of the long-reads mapper.

Finally, we aimed to estimate the portion of artifacts arising at the sonication step. As described previously, random sonication may result in different fragments originating from similar copies of long proximity ligation products (Figure 2B). In ONT reads, we were able to count indirect junctions of DNA fragments, i.e. when two DNA fragments are separated by a third fragment. Such indirectly interacting fragments may be considered as directly interacting after sonication and Illumina-sequencing if read length is not sufficient to detect an intervening DNA fragment. We found that exclusion of such indirect contacts reduces the number of artifacts only slightly (from 5,67% to 5,61%), indicating that this source of artifacts is not essential.

4. Discussion

Our data shows that PCR-based scHi-C protocols provide better data quantity and quality compared to MDA-based protocols. The vast majority of artifacts observed in MDA data arise from phi29 polymerase template switching. Random sonication does not add much to the number of the artifacts. Long-read sequencing makes it possible to find products of circular overamplification and distinguish between direct and indirect contacts. However, accurate aligning of long chimeric reads is challenging, and segment alignments must be carefully filtered to avoid artifacts.

We recommend to use PCR-based strategy for single-cell Hi-C protocols. However, in some cases MDA might be required: for example, if the amount of the input material is too low, or if recovery of contacts is paramount. In addition, combining MDA with long-read sequencing allows detecting multi-way, long-range interactions (Ulahannan et al., 2019; Tavares-Cadete et al., 2020). In these and other cases when MDA is required, we suggest filtering reads junctions based on the distance to the expected genomic cut site. We note that other strategies of chimeric MDA reads detection (Tu et al., 2015, 2017; Lu et al., 2019) are less applicable to Hi-C data, due to chimeric nature of typical Hi-C reads.

Declarations

Author contribution statement

Maria Gridina: Conceived and designed the experiments; Performed the experiments; Wrote the paper.

Alena Taskina, Timofey Lagunov: Analyzed and interpreted the data; Wrote the paper.

Artem Nurislamov: Performed the experiments; Wrote the paper.

Tatiana Kulikova, Alla Krasikova, Veniamin Fishman: Conceived and designed the experiments; Contributed reagents, materials, analysis tools or data; Wrote the paper.

Funding statement

This work, including cells isolation and NGS library preparation, was supported by Russian Science Foundation grant #20-64-46021. Illumina sequencing was performed by Skoltech Genomics Core Facility and BGI Sequencing Facilities. Long-read sequencing was performed using equipment of the Novosibirsk State University, supported by the Ministry of Education and Science of Russian Federation, grant #2019-0546 (FSUS-2020-0040). ONT data analysis was performed on the nodes of HPC cluster of the Institute of Cytology and Genetics, supported by the project No. 121031800061-7). Illumina data analysis was supported by strategic academic leadership program “Priority 2030” in Novosibirsk State University.

Data availability statement

Data associated with this study has been deposited at NCBI SRA under the accession number PRJNA834620.

Declaration of interest's statement

The authors declare no conflict of interest.

Additional information

No additional information is available for this paper.

References

Borgström, E., Paterlini, M., Mold, J.E., Frisen, J., Lundeberg, J., 2017. Comparison of whole genome amplification techniques for human single cell exome sequencing. PLoS One 12, e0171566.

Collombet, S., Ranisavljevic, N., Nagano, T., Varnai, C., Shisode, T., Leung, W., et al., 2020. Parental-to-embryo switch of chromosome organization in early embryogenesis. Nature 580, 142–146.

Chen, M., Song, P., Zou, D., Hu, X., Zhao, S., Gao, S., et al., 2014. Comparison of multiple displacement amplification (MDA) and multiple annealing and looping-based amplification cycles (MALBAC) in single-cell sequencing. PLoS One 9, e114520.

Dean, F.B., Hosono, S., Fang, L., Wu, X., Faruqi, A.F., Bray-Ward, P., et al., 2002. Comprehensive human genome amplification using multiple displacement amplification. Proc. Natl. Acad. Sci. USA 99, 5261–5266.

Díaz, N., Kruse, K., Erdmann, T., Staiger, A.M., Ott, G., Lenz, G., et al., 2018. Chromatin conformation analysis of primary patient tissue using a low input Hi-C method. Nat. Commun. 9, 4938.

Fishman, V., Battulin, N., Nuriddinov, M., Maslova, A., Zlotina, A., Strunov, A., et al., 2019. 3D organization of chicken genome demonstrates evolutionary conservation of topologically associated domains and highlights unique architecture of erythrocytes' chromatin. Nucleic Acids Res. 47, 648–665.

Flyamer, I.M., Gassler, J., Imakaev, M., Brandão, H.B., Ulianov, S.V., Abdennur, N., et al., 2017. Single-nucleus Hi-C reveals unique chromatin reorganization at oocyte-to-zygote transition. Nature 544, 110–114.

Galitsyna, A.A., Gelfand, M.S., 2021. Single-cell Hi-C data analysis: safety in numbers. Briefings Bioinf. 22, bbab316.

Gridina, M., Mozheiko, E., Valeev, E., Nazarenko, L.P., Lopatkina, M.E., Markova, Z.G., et al., 2021. A cookbook for DNase Hi-C. Epigenet. Chromatin 14, 15.

Huang, L., Ma, F., Chapman, A., Lu, S., Xie, X.S., 2015. Single-cell whole-genome amplification and sequencing: methodology and applications. Annu. Rev. Genom. Hum. Genet. 16, 79–102.

Ke, Y., Xu, Y., Chen, X., Feng, S., Liu, Z., Sun, Y., et al., 2017. 3D chromatin structures of mature gametes and structural reprogramming during mammalian embryogenesis. Cell 170, 367–381.e20.

Kempfer, R., Pombo, A., 2020. Methods for mapping 3D chromosome architecture. Nat. Rev. Genet. 21, 207–226.

Krasikova, A., Khodyuchenko, T., Maslova, A., Vasilevskaya, E., 2012. Three-dimensional organisation of RNA-processing machinery in avian growing oocyte nucleus. Chromosome Res. 20, 979–994.

Kumar, G., Garnova, E., Reagin, M., Vidali, A., 2008. Improved multiple displacement amplification with φ29 DNA polymerase for genotyping of single human cells. Biotechniques 44, 879–890.
Lasken, R.S., Stockwell, T.B., 2007. Mechanism of chimera formation during the multiple displacement amplification reaction. BMC Biotechnol. 7, 19.
Lu, N., Li, J., Bi, C., Guo, J., Tao, Y., Luan, K., et al., 2019. ChimeraMiner: an improved chimeric read detection pipeline and its application in single cell sequencing. Int. J. Mol. Sci. 20, 1953.
Nagano, T., Lubling, Y., Várnai, C., Dudley, C., Leung, W., Baran, Y., et al., 2017. Cell-cycle dynamics of chromosomal organization at single-cell resolution. Nature 547, 61–67.
National Research Council, 2011. Guide for the Care and Use of Laboratory Animals, eighth ed. Natl. Acad. Press, p. 12910.
Stevens, T.J., Lando, D., Basu, S., Atkinson, L.P., Cao, Y., Lee, S.F., et al., 2017. 3D structures of individual mammalian genomes studied by single-cell Hi-C. Nature 544, 59–64.
Tan, L., Xing, D., Chang, C.-H., Li, H., Xie, X.S., 2018. Three-dimensional genome structures of single diploid human cells. Science 361, 924–928.
Tavares-Cadete, F., Norouzi, D., Dekker, B., Liu, Y., Dekker, J., 2020. Multi-contact 3C reveals that the human genome during interphase is largely not entangled. Nat. Struct. Mol. Biol. 27, 1105–1114.
Tu, J., Guo, J., Li, J., Gao, S., Yao, B., Lu, Z., 2015. Systematic characteristic exploration of the chimeras generated in multiple displacement amplification through next generation sequencing data reanalysis. PLoS One 10, e0139857.
Tu, J., Lu, N., Duan, M., Huang, M., Chen, L., Li, J., et al., 2017. Hotspot selective preference of the chimeric sequences formed in multiple displacement amplification. Int. J. Mol. Sci. 18, 492.
Ulahannan, N., Pendleton, M., Deshpande, A., Schwenk, S., Behr, J.M., Dai, X., et al., 2019. Nanopore sequencing of DNA concatemers reveals higher-order features of chromatin structure. Genomics.
Ulianov, S.V., Zakharova, V.V., Galitsyna, A.A., Kos, P.I., Polovnikov, K.E., Flyamer, I.M., et al., 2021. Order and stochasticity in the folding of individual Drosophila genomes. Nat. Commun. 12, 41.
Zhang, K., Wu, D.-Y., Zheng, H., Wang, Y., Sun, Q.-R., Liu, X., et al., 2020. Analysis of genome architecture during SCNT reveals a role of cohesin in impeding minor ZGA. Mol. Cell 79, 234–250 e9.